Jurnal Polimesin
Department of Mechanical Engineering
State Polytechnic of Lhokseumawe
http://e-jurnal.pnl.ac.id/polimesin

e-ISSN : 2549-1999 No. : 3 Month : June
p-ISSN : 1693-5462 Volume : 24 Year : 2026

Processing dates: received on 2025-10-31, reviewed on 2026-1-14, accepted on 2026-05-19 and online availability on 2026-06-30

Performance and emission analysis of a Komatsu PC195LC common-rail diesel engine under injector type and spray-angle variations

Yosephus Ardean Kurnianto Prayitno[1,2], Sugiyanto[1,2*], Ilham Ayu Putri Pratiwi[1,2], Braam Delfian Prihadianto[1], Muhammad Fauzan[1], Setyawan Adi Nugraha[1], Josua Aditya Manuel[3], Sutikno[3], and Muhammad Novan Budi Prasetya[3]

[1]Department of Mechanical Engineering, Vocational School, Gadjah Mada University, Yogyakarta 55281, Indonesia
[2]Pusat Studi Energi (Center for Energy Studies), Gadjah Mada University, Yogyakarta 55281, Indonesia
[3] PT. United Tractors, Tbk, Semarang, Indonesia
*Corresponding author: yosephus.ardean@ugm.ac.id

Abstract

Injector condition and spray characteristics strongly influence fuel atomization, combustion efficiency, and exhaust emissions in common-rail diesel engines. This study aims to evaluate the performance and emission responses of a Komatsu PC195LC diesel engine under variations in injector type and spray angle by integrating field measurements with bench-scale spray characterization. Two injector types (OEM vs local) were tested at 1050, 1500, and 2050 rpm; fuel rate and specific fuel consumption were logged over two-minute windows, and post-operation (3000 h) inspections assessed wear. A back-lit imaging rig measured spray angle and droplet distribution at 50 and 100 bar; a simple mixing–atomization model linked spray metrics to air–fuel preparation. Field results show the OEM injector reduced fuel rate by 0.78 L/h (3.45%) versus the local unit under the duty cycle tested. Bench data indicate wider spray angles and finer droplets at higher pressure, consistent with improved mixture formation. Joint analysis attributes the observed SFC gains to healthier nozzle geometry and spray targeting. The study provides guidance on injector selection, condition monitoring, and pressure/angle calibration towards Euro-4-aligned efficiency and emissions.

Keywords:
Engine performance, emission, injector type, spray angle, excavator, PC-195LC

1 Introduction

Heavy-duty excavators remain central to mining, construction, and large-scale earth-moving activities, forming a substantial fraction of non-road mobile machinery (NRMM) fleets worldwide. Field measurements and inventory-based analyses indicate that construction machinery fleets contribute significantly to urban and regional emissions due to high fuel consumption and prolonged operational lifetimes, with relatively slow fleet turnover compared to on-road vehicles [8], [9].

Their duty cycles, which are heavily dominated by high-amplitude transients, low-load manoeuvring, and high-torque digging phases, make the fuel system a primary lever for both operating cost optimization and environmental footprint mitigation. In heavy excavation environments, achieving optimal powertrain efficiency requires complex, transient power-matching co-dependencies between the diesel engine governor and the hydraulic transmission circuit [10]. This operational stress is further pronounced under aggressive alternative fuel mandates, where real-time fleet health monitoring systems indicate that high-percentage biodiesel blends (such as B40) impose significant durability and component-degradation constraints on the high-pressure fuelling loop [11]. Within these compression-ignition architectures, macroscopic mixture formation, ignition quality, and pollutant precursors are fundamentally governed by injection timing, rate shaping, and near-field spray development inside the cylinder [12]. At the micro-component level, these processes are easily disrupted by the high-temperature environment of the combustion chamber, which triggers internal nozzle fouling and carbonaceous deposit growth [13]. This internal coking constriction distorts localized boundary layer flow, induces unstable hole-to-hole string cavitation, and leads to collapsed spray angle cones and altered droplet atomization mechanics [14]. While full multidimensional computational fluid dynamics (CFD) capture these flow detachments, the deployment of cross-sectionally averaged, reduced-order reactive spray surrogates has emerged as a computationally efficient alternative for rapid condition screening and mixing-index calibration [15]. In modern common-rail systems, injector hardware is based on its type, nozzle health, internal hydraulics, and spray characteristics such as cone angle, stability, and droplet size distribution, and critical shape charge preparation. Here, the rail-pressure management and nozzle geometry directly modulate these outcomes [12], [16], in which canonical spray is used to model the coupling between breakup, atomization, and evaporation that drives burn completeness [2], [3], [17].

In mining fields, injector configuration decisions are frequently constrained by availability and cost considerations. However, the macroscopic spray characteristics governed by injector geometry and internal hydraulics significantly influence mixture formation and combustion behaviour under realistic duty profiles. Variations in nozzle condition and injection parameters modify spray penetration, cone angle, and droplet size distribution, thereby affecting air–fuel preparation and subsequent combustion efficiency [1], [2], [3], [18]. Given duty cycles characterized by frequent transients, low-speed manoeuvring, and high-torque digging, the fuel injection system becomes a primary determinant of both operating cost and environmental footprint. Within compression-ignition architectures, mixture formation, ignition quality, and pollutant precursor formation are governed by injection timing, rate shaping, and spray development inside the cylinder [12]. In modern common-rail systems, injector hardware including nozzle geometry, internal hydraulics, and spray characteristics such as cone angle, stability, and droplet size distribution, and critically shaped charge preparation. Rail-pressure management and nozzle design directly modulate these outcomes, and injection pressure has been experimentally linked to spray development and atomization behaviour in direct-injection systems [18], [19], while canonical spray formulations capture the coupling between breakup, atomization, evaporation, and combustion completeness [17].

2 Research methodology

In order to address these gaps, this study integrated (i) field measurements on a Komatsu PC195LC common-rail excavator to evaluate fuel rate, SFC, and emission indicators across representative operating points for two injector types (OEM vs local), with (ii) bench characterization of spray angle and droplet distribution under controlled injection pressures, linked through a compact mixing–atomization model to infer air–fuel preparation quality. Platform context and duty expectations are taken from manufacturer/market documentation for the 20-ton class, while emission indicators are derived using established diesel emission calculation methodologies based on exhaust mass flow and concentration measurements [20]. The analysis is interpreted with reference to Euro-aligned efficiency and cooling/emissions objectives pertinent to heavy-duty diesel equipment [21].

The study is performed in two main stages, which are the numerical simulation and experimental investigations. In the first

stage, the spray angle effect was investigated with focuses on bench spray simulation and literature study. In the second stage, experiments were conducted to obtain the fuel rate and specific fuel consumption (SFC). In addition, emission data were taken to validate the excavator's performance.

2.1 Numerical simulation

To support the experimental analysis and to enable systematic comparison between injector conditions, a reduced-order numerical surrogate of diesel spray behaviour was developed (see Fig. 1). The objective of this simulation was not to resolve detailed internal nozzle flow or multiphase turbulence, but to preserve two experimentally observable macroscopic trends:

(i) spray plume widening with increasing injection pressure
(ii) finer atomization for a healthy (clean) injector relative to an abnormal (coked) injector at the same operating condition.

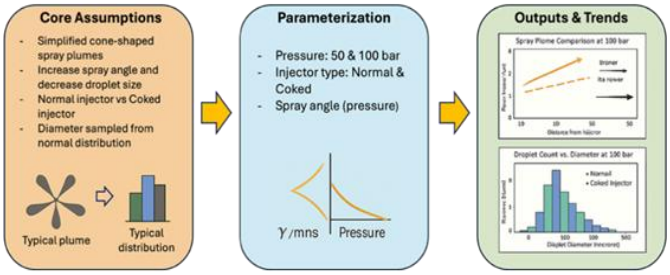

Fig. 1. Simulation schematic diagram

The surrogate is intentionally lightweight and transparent, allowing parametric sweeps and direct linkage between spray metrics and a qualitative mixing index.

The spray was represented as a two-dimensional conical plume characterised by a half-angle θ, with geometric bounds defined as $y = \pm \tan(\theta)\, x$. Spray penetration, air entrainment, evaporation, and wall interaction were not solved, as the present analysis focuses exclusively on plume geometry and droplet size statistics as first-order indicators of mixture preparation. Injection pressure effects were represented using the effective pressure drop across the nozzle, $\Delta P = P_{\text{inj}} - P_{\text{amb}}$, which governs injection velocity through Bernoulli-type scaling, consistent with established diesel spray theory [1], [2], [3]. The spray half-angle θ is represented using a bounded sublinear surrogate as follows.

$$\theta(P) = \theta_{min} + (\theta_{max} - \theta_{min})(1 - e^{-k\sqrt{\Delta P}}) \qquad (1)$$

where $\Delta P = P_{\text{inj}} - P_{\text{amb}}$ is the effective pressure drop across the nozzle. The $\sqrt{\Delta P}$ dependence is consistent with Bernoulli-type injection-velocity scaling, while the exponential term enforces an asymptotic ceiling that reflects geometric and internal-flow limits on plume widening. The parameters $\theta_{\min}$, $\theta_{\max}$, and k are treated as injector-condition-dependent calibration constants (e.g., normal vs coked), enabling a simple but physically plausible mapping between pressure and plume spreading over the 50–100 bar range (see Fig. 2).

In diesel spray systems, jet momentum, breakup intensity, and turbulence scale sub-linearly with injection velocity, and spray angle development is influenced by nozzle geometry, internal flow structure, cavitation, and ambient density effects [1], [16], [18]. Accordingly, the spray half-angle was modelled as a bounded sublinear function of $\sqrt{\Delta P}$, reflecting diminishing widening once geometric and flow constraints are reached. Such behaviour is consistent with experimentally observed cone-angle responses under varying injection pressures reported in high-pressure diesel spray studies [18], [19]. In the limited pressure range considered (50–100 bar), this response reduces to a quasi-linear trend suitable for comparative visualization and injector-condition screening.

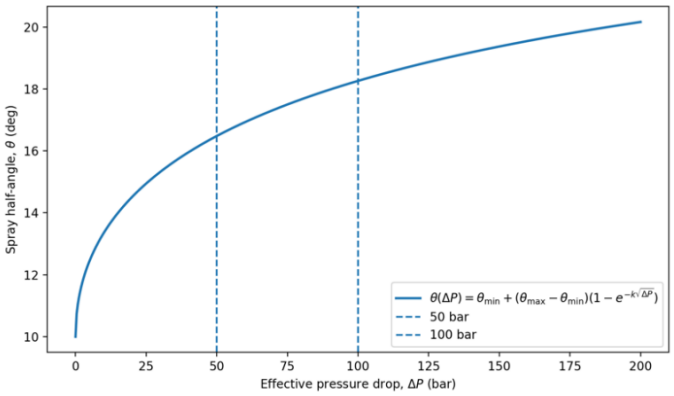

Fig. 2. Bounded sub-linear spray-angle surrogate.

Droplet size was treated statistically using a simplified probability distribution, serving as a proxy for relative atomization quality rather than an explicit primary- and secondary-breakup model. Although realistic diesel sprays typically follow lognormal or Rosin–Rammler distributions [1], [2], droplet diameters in this surrogate were sampled from a truncated normal distribution whose mean decreases with increasing ΔP, reflecting improved atomization at higher injection pressure. Differences between clean and coked injectors were introduced through shifts in distribution mean and variance, with degraded nozzles producing coarser droplets and heavier large-diameter tails, consistent with impaired breakup behaviour reported in experimental spray characterization studies [18], [19].

Two representative injection pressures, 50 bar and 100 bar, were selected to represent low and high pressure regimes commonly used in bench spray characterization. These operating points enable direct comparison with back-lit imaging data and provide a physically interpretable bridge between spray geometry and engine-level performance indicators. Hence, to simulate these conditions,

2.2 Experimental investigations

2.2.1 Experimental setup

Fig. 3 shows the excavator Komatsu PC195LC which has a typical fuel system based on common rail for its diesel engines (Fig. 4). The Komatsu PC195LC was widely utilized as an efficient alternative in the 20-ton excavator class, offering notable advantages in fuel economy and operational efficiency (see Table 1). The unit is powered by a diesel engine, which provides superior thermal efficiency, higher compression ratio, greater torque output, and enhanced durability compared to conventional gasoline engines [22], [23], [24]. The diesel engine operates through four combustion strokes, which are intake, compression, power, and exhaust. These four combustion strokes collectively ensure effective energy conversion. In this model, the engine was equipped with a common-rail fuel injection system, enabling more precise fuel delivery and optimized combustion relative to traditional mechanical - injection systems. The common-rail fuel pathway extends from the fuel tank through the high-pressure pump and rail to the injector, ensuring stable fuel pressure and consistent injection across all cylinders.

Fig. 3. Excavator PC195LC [6].

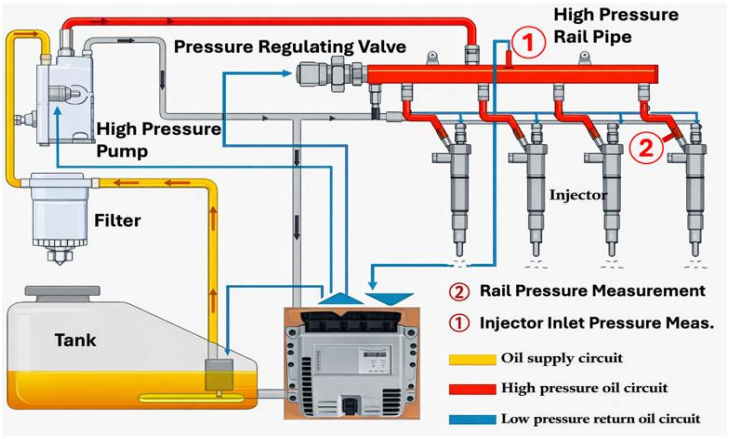

Fig. 4. Fuel system of common rail diesel engine.

In order to investigate the performance of the excavator PC195LC diesel engine, a comparative mixed-method study was conducted. The study quantifies how injector type (OEM vs. local) and spray angle affect fuel rate, SFC, and emission indicators through three aspects, which were field trials, bench spray simulation, and a compact mixing–atomization analysis. Here, the experimental condition was run as follows:

- Single type of Excavator, Komatsu PC195LC
- Two matched injector sets: OEM and local
- Single Batch Biodiesel B40 Fuel (±2 °C), and
- Three rpm variations: 1,050/1,500/2,050.

The rpm variations of 1050, 1500, and 2050 rpm were selected to represent three practically relevant operating conditions of the Komatsu PC195LC excavator. The 1050 rpm point was used as an idle or near-idle baseline with minimal hydraulic demand [4]. While, the 1500 rpm point was used to represent partial-load operation, particularly sloping and trenching, because this speed lies in the engine's torque-dominant region [4]. The 2050 rpm point was used to represent near-rated high-load operation associated with digging-stocking and loading-unloading cycles, in which operators typically maintain high engine speed to preserve hydraulic responsiveness and productivity [4]. This speed represents the upper operational ceiling governed by the manufacturer's factory ECU settings for the SAA4D107E-1 engine configuration; hence, higher speed variations are restricted to prevent mechanical over-speeding and hydraulic system degradation. Thus, the classification was important as representative operation based on the actual excavator loading, which is governed by the combined effects of engine speed, hydraulic demand, operator input, and material resistance. Thus, this classification consistently distinguishes idling, trenching, and loading as separate major work states [5].

Table 1. Excavator komatsu PC195LC specifications

Item	Value
Engine Model	SAA4D107E-1
Engine Type	4-cycle, water cooled, in-line, direct injection, with turbocharger and after cooler
Number Of Cylinder	4
Piston Displacement	4,460 L
Piston Broke	124 mm
Cylinder Bore	107 mm
Net Engine Output	123 HP
Compression pressure test value	Min. 2.41 MPa, Min. Operation 1.69 MPa {17.2 kg/cm²}

The combustion efficiency of a diesel engine is determined using the specific fuel consumption (SFC), which represents the mass flow rate of fuel per unit of power output produced by the engine [12]. A lower SFC value indicates a more efficient combustion process, as less fuel is required to generate the same power compared to an engine with a higher SFC. The relationship defining SFC can be expressed mathematically as shown in Equation (2).

$$SFC = \frac{\dot{m}_f}{D} \tag{2}$$

where $\dot{m}_f$ is the mass flow rate of the fuel (kg/hour) and D is the power generated from the diesel engine (kW).

Next, the specific emission equation (g/kWh) was used to quantify the amount of exhaust gas emitted per unit of energy output produced by the engine. This parameter was essential for evaluating engine efficiency, as it reflected the relationship between the amount of exhaust emissions and the corresponding energy generation. The specific emission relationship was expressed in Equation (3) [20], [25].

$$em = \frac{q \times 3600}{D} \tag{3}$$

where em is the specific power emission in g/kWh and q is the exhaust gas flow rate (g/s).

To specifically measure the SFC and the corresponding engine output power, the KOMTRAX system was utilized to obtain real-time operational parameters from the excavator [6]. Meanwhile, exhaust gas emissions were measured using a portable flue gas analyzer (MRU VARIOluxx) [7]. The analyzer operates using a combination of electrochemical sensors and non-dispersive infrared (NDIR) technology, enabling simultaneous measurement of major exhaust gas components including O_2, CO, CO_2, NOx, and SO_2. The sampling system consists of a probe inserted into the exhaust stream, followed by gas conditioning through a Peltier-based gas cooler, particulate filtration, and controlled pumping to ensure stable and accurate measurement. In addition to gas concentration, the analyzer records flue gas temperature, pressure, and flow-related parameters, allowing further normalization and conversion into mass-based emission units such as mg/Nm³ [7].

Field trials were executed by capturing real-time operational parameters over a continuous, steady-state logging window of two minutes for each operational variation based on KOMTRAX system. Data acquisition was executed at a sampling rate of 1 Hz, accumulating a total sample size of n=120 data points per operational mode to ensure statistical representation. Data dispersion and transient engine governor variations were quantified explicitly using standard deviation error bars σ.

3 Result and discussion

3.1 Spray angle to pressure characteristics

Two patterns of spray angle to pressure were successfully observed to define the characteristics of injectors by transparent surrogate of diesel-spray behaviour: (i) spray plumes widen as rail pressure increases and (ii) abnormal (coked) nozzles exhibit reduced plume opening and coarser atomization relative to clean nozzles. In this baseline run, the spray half-angle was mapped to pressure with a simple linear law (for visualization only), and plumes were rendered as conical envelopes. Thus, a first-order representation consistent with the hollow-cone pattern of the PC-195LC injector family. Droplet diameters were sampled from a truncated normal distribution whose mean scales inversely with pressure, reflecting finer atomization at higher ΔP. No penetration, evaporation, or wall-interaction ODEs were solved; instead, the model isolates geometry and size statistics to support qualitative comparison.

At 50 bar (Fig. 5), the clean injector produces a visibly wider cone than the coked injector, while both remain relatively narrow at short axial distances. At 100 bar (Fig. 6), the envelopes further open and the gap between clean and coked becomes more evident, which is more consistent with partial-orifice blockage dampening the angle response. The droplet histograms corroborate the geometric trend: at 50 bar (Fig. 4) the diameter distributions centre around larger medians with broad variance; at 100 bar (Fig. 5) both distributions

shift toward smaller medians, indicating finer atomization at higher pressure. Across pressures, the coked injector retains a slightly larger median and a heavier right tail, i.e., larger droplets, which is consistent with impaired breakup. The greater spread observed in the distributions is expected from the hollow-cone abstraction and would further broaden when wall interaction and secondary breakup are active; in practical chambers, impingement can promote additional breakup, altering both tail behaviour and effective cone development.

As explained before, Figures 5 and 6 show a trend in which abnormal/coked injectors yield narrower spray angles than clean injectors at the same pressure. Here, the opposite of a healthy widening response is producing a more confined plume. On the other hand, higher pressure reduces the characteristic droplet size (median shifts lower) for both injectors, but the coked nozzle remains coarser and exhibits a heavier large-droplet tail. This localized phenomenon matches experimental characterizations of high-pressure coked diesel hardware, where inner orifice restriction and carbonaceous layers disrupt velocity profiles and inhibit the typical atomization enhancements expected at higher rail pressures [13]. Furthermore, as detailed in recent multi-hole injector reviews, internal foulants trigger unstable hole-to-hole string cavitation and string flow detachments that directly collapse macro cone angles while shifting droplet distributions toward larger diameters [14]. In addition, the conical spread approximation captures first-order geometry for hollow-cone sprays; however, wall interaction and evaporation (omitted) would intensify secondary aerodynamic breakup and may further differentiate the tails. Implementing cross-sectionally averaged reactive spray frameworks indicates that while low-order surrogates are highly efficient for primary screening, the integration of ambient gas density fields and secondary evaporation layers is crucial to capture transient droplet-to-air shear limits over extended domains [15].

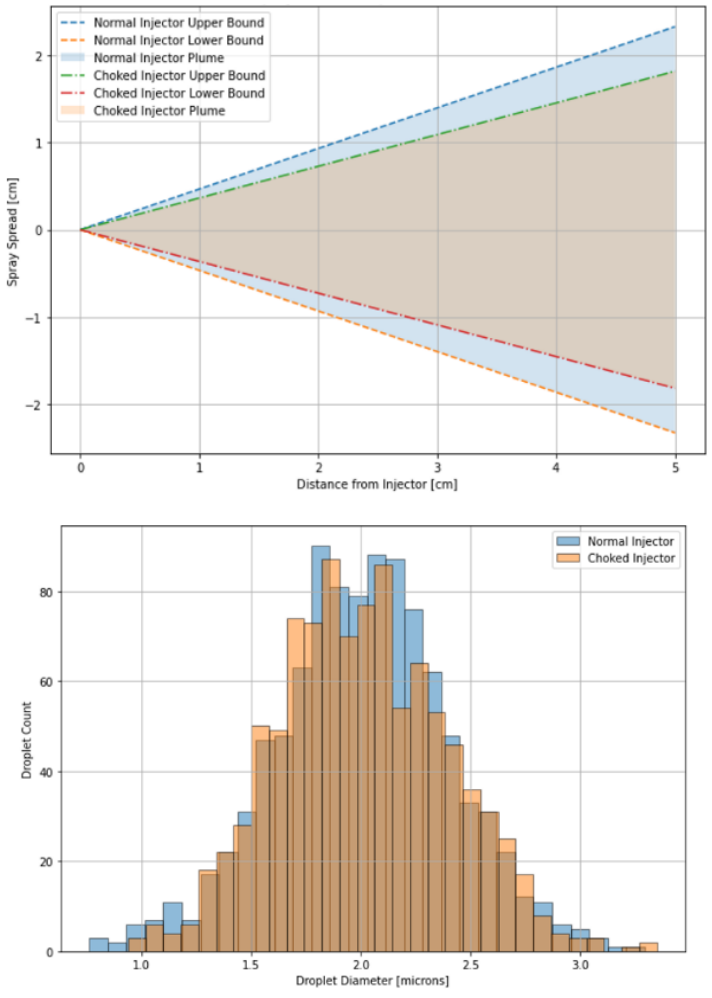

Fig. 5. Spray angle to droplet distributions under 50 bar pressure.

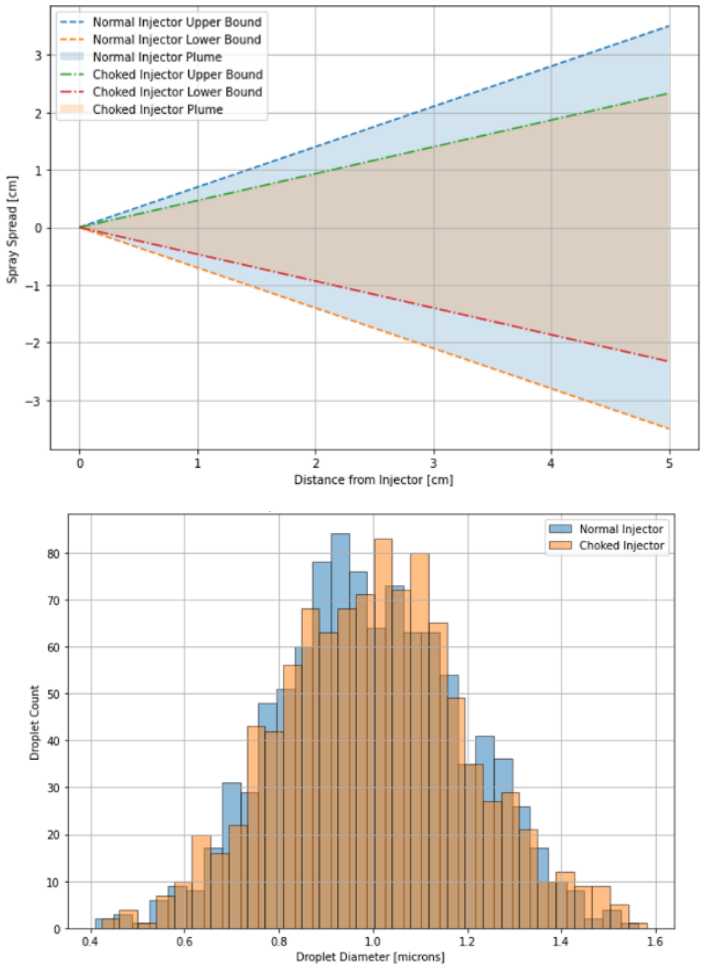

Fig. 6. Spray angle to droplet distributions under 100 bar pressure.

3.2 Specific fuel consumption

The genuine Komatsu (OEM) injector demonstrated a slightly lower fuel consumption rate compared to the local injector. This finding indicates that at higher engine speeds, the OEM injector offers better fuel efficiency, achieving a reduction of approximately 0.78 L h^{-1}. Across speed ranges, the OEM injector consumed 7.10% less fuel at medium speed and 3.45% less at high speed than the local injector (see Fig. 7).

The specific fuel consumption (SFC) values measured for both injectors were nearly identical, suggesting that the combustion efficiency per unit power output was comparable between the two systems. This finding aligns with optimization-driven power transmission designs where rigid hydraulic circuit configurations dictate a uniform, fuel-efficient load matching under steady conditions [10]. Nonetheless, the OEM injector exhibited a superior overall performance, as its post-operation measurements after approximately 3,000 operating hours (HM) remained closely aligned with those of a newly installed local injector. This outcome highlights the durability and stable efficiency of the OEM injector under prolonged operational conditions (see Fig. 8). This outcome highlights the durability and stable efficiency of the OEM injector under prolonged operational conditions. Longitudinal fleet studies on heavy industrial systems confirm that genuine common-rail architectures maintain their component-level integrity far better against the accelerated deposit-forming tendencies and mechanical wearing effects of biodiesel blends, preventing the severe fuel-rate and efficiency degradation often captured via automated health-monitoring frameworks in lower-grade alternatives after extended service lifetimes [11], [18], [26], [27].

To ensure the statistical validity and repeatability of the engine trials, a high-density data collection approach was utilized. The operational parameters were logged continuously across 120 discrete samples (n = 120) for each operational state. The synthesized statistical profile of the field measurement data, which details the

exact arithmetic means and standard deviations (σ) for both the OEM and local fuel injector tracks, is summarized in Table 2 before being evaluated graphically in Fig. 7 and Fig. 8.

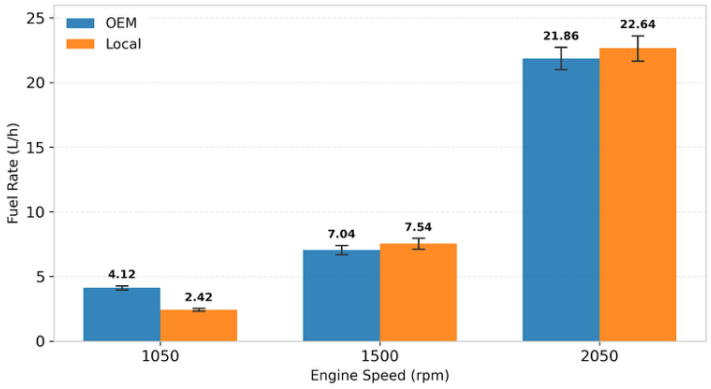

Fig. 7. Fuel rate between two injector types over different engine speed.

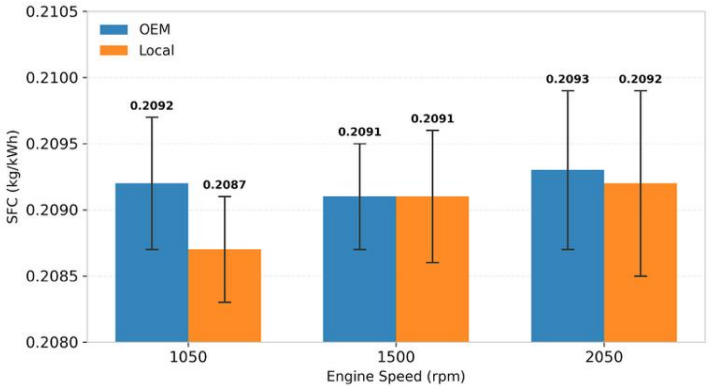

Fig. 8. SFC between two injector types over different engine speed.

Table 2. Statistical summary matrix of excavator common-rail fuel system parameters

Engine Speed (rpm)	SFC Std. Dev σ (kg/kWh)	Fuel Rate Std. Dev σ (L/h)
1050 [OEM]	0.0005	0.15
1050 [Local]	0.0004	0.10
1500 [OEM]	0.0004	0.35
1500 [Local]	0.0005	0.42
2050 [OEM]	0.0006	0.85
2050 [Local]	0.0007	0.98

3.3 Emission

Both injectors exhibited CO and NOx emission levels below the Euro 4 standard, indicating that the use of either the local or genuine Komatsu (OEM) injector in the PC195LC excavator remains environmentally compliant (see Fig. 9). This finding aligns with Sustainable Development Goal (SDG) No. 13 – Climate Action, demonstrating that both injector types contribute to reduced environmental impact through cleaner combustion performance. The measured O_2 concentration exceeded 15% for both injectors, which may suggest possible issues with the intake manifold or oxygen sensor of the unit. Elevated O_2 levels can disrupt the air–fuel ratio balance, leading to incomplete combustion. This is further supported by the relatively high CO concentration, a by-product typically associated with incomplete oxidation of carbon during combustion.

In contrast, the SO_2 content in the exhaust gases for both injectors remained low, confirming that the fuel quality used in this test was high and free from excessive sulphur contamination. Overall, these results indicate that while both injectors operate within clean-emission limits, maintenance of the air-intake and sensor systems is crucial to ensure optimal combustion efficiency.

The findings indicate that the use of two different injector types was not able to produce a significant difference in terms of fuel efficiency or exhaust gas emissions. Nevertheless, the OEM injector exhibited slightly superior performance, maintaining stable operation even after approximately 3,000 operating hours (HM). At high engine speeds, the OEM injector demonstrated a 3.45% improvement in fuel-rate efficiency compared with the local injector. The exhaust emission content between the two injectors showed no significant variation, and the measured CO and NOx concentrations for both remained below the Euro 4 threshold, indicating compliance with current emission standards. However, the observed oxygen (O_2) content exceeding 15% suggests possible air–fuel imbalance that may lead to incomplete combustion. This issue is likely related to a malfunction in the intake manifold system or oxygen sensor, which should be further inspected to ensure proper combustion efficiency.

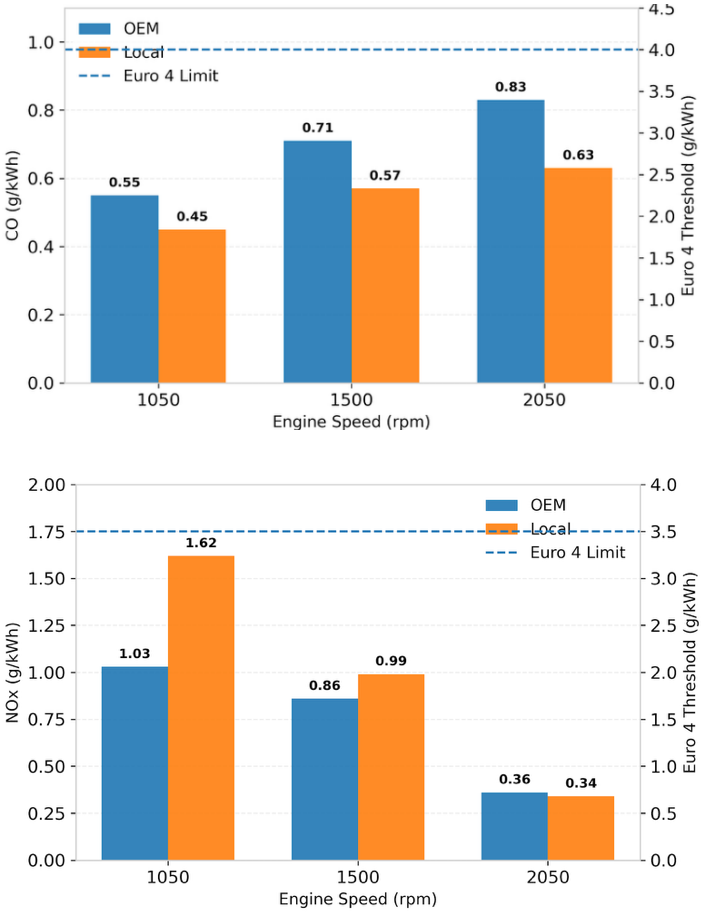

Fig. 9. CO and NOx emission between two injector types over different engine speed.

A visual inspection of the OEM injector revealed surface wear on the injector body after 3,000 hours of operation, attributed to mechanical friction during prolonged use [28], [29], [30]. Such wear is typical for components operating under high pressure and extended service hours. To maintain optimal performance, it is recommended that the OEM injector be evaluated on a test bench and that injector assembly replacement be conducted during the 6,000-hour midlife service interval .

Routine fuel system maintenance plays a crucial role in extending injector life. The quality of fuel and the integrity of fuel filters must be carefully managed, as biodiesel blends commonly used in heavy equipment can form gel-like deposits that degrade fuel-system components [20], [31]. Fuel filters serve as a primary defence against such contamination and should be replaced during periodic maintenance every 500 hours to prevent impurities from reaching the injector assembly and to ensure consistent engine performance and reliability.

4 Conclusion

This work demonstrates a performance and emission responses to injector type and spray-angle variation in the Komatsu PC195LC Common-Rail Diesel Engine. According to the result, the main conclusions are as follows:

a. Stage 1: The bounded, sublinear transparent numerical surrogate successfully differentiates injector nozzle health and rail-pressure development. Higher effective pressure drops open the simulated spray cone envelope and reduce droplet sizes, indicating improved charge preparation. Conversely, the coked injector model effectively captures orifice-constriction mechanics, displaying a narrower plume spread and a heavier large-diameter droplet tail that signifies impaired fuel atomization.
b. Comparative testing of the genuine Komatsu (OEM) and local injectors revealed comparable fuel efficiency and emission performance, with the Komatsu unit showing slightly better fuel-rate efficiency (3.45%) at high speed and maintaining stable operation after 3,000 hours, confirming its superior durability.
c. Stage 2: Steady-state field logging (n=120 per mode) verified that the genuine OEM common-rail track achieves a 3.45% fuel-rate efficiency improvement over the local alternative under high-load conditions (2050 rpm), confirming superior durability after 3,000 hours of operation. Data variance and standard deviations (σ) naturally increased with engine speed due to transient hydraulic digging demands. Both injector tracks remain fully compliant with Euro 4 emission thresholds for CO and NO_x. However, exhaust oxygen O_2 (>15%) indicates minor air–fuel path imbalances, reinforcing that strict adherence to a 500-hour fuel-filter replacement interval is essential to mitigate biodiesel-related deposits and ensure long-term combustion integrity.

These findings provide practical references for injector diagnostics, maintenance scheduling, and spray optimization in common-rail diesel excavator systems. Future research should focus on expanding the model to incorporate nonlinear pressure–angle correlations, secondary breakup, and wall interaction dynamics.

Aknowledgments

This study is partially funded by the Sekolah Vokasi UGM 2025 Research Grant and by the collaborative research program between PT. United Tractors, Tbk. and Heavy Equipment Management and Maintenance Engineering, Department of Mechanical Engineering, Sekolah Vokasi, Universitas Gadjah Mada. This study is also part of the work done by the Heavy Vehicle Research and Training Center, UGM, Indonesia.

References

[1] J. V. Pastor, J. Javier López, J. M. García, and J. M. Pastor, "A 1D model for the description of mixing-controlled inert diesel sprays," Fuel, vol. 87, no. 13–14, pp. 2871–2885, 2008, doi: 10.1016/j.fuel.2008.04.017.

[2] H. J. Kim, S. H. Park, and C. S. Lee, "A study on the macroscopic spray behavior and atomization characteristics of biodiesel and dimethyl ether sprays under increased ambient pressure," Fuel Processing Technology, vol. 91, no. 3, pp. 354–363, Mar. 2010, doi: 10.1016/j.fuproc.2009.11.007.

[3] F. dos Santos and L. le Moyne, "Spray atomization models in engine applications, from correlations to direct numerical simulations," Oil and Gas Science and Technology, vol. 66, no. 5, pp. 801–822, Sep. 2011, doi: 10.2516/ogst/2011116.

[4] Komatsu, Shop Manual PC195LC-8_LEBMP19800. 2016.

[5] A. Molaei, A. Kolu, K. Lahtinen, and M. Geimer, "Automatic recognition of excavator working cycles using supervised learning and motion data obtained from inertial measurement units (IMUs)," Construction Robotics, vol. 8, no. 2, Dec. 2024, doi: 10.1007/s41693-024-00130-0.

[6] Tbk. PT. United Tractors, Komatsu PC195LC-8 Hydraulic Excavator. 2017.

[7] MRU, VARIOluxx SYNGAS USER MANUAL, 2024th-04–23rd ed. 2023.

[8] C. D. Desouza, D. J. Marsh, S. D. Beevers, N. Molden, and D. C. Green, "Real-world emissions from non-road mobile machinery in London," Atmos. Environ., vol. 223, Feb. 2020, doi: 10.1016/j.atmosenv.2020.117301.

[9] X. Li et al., "Emissions of air pollutants from non-road construction machinery in Beijing from 2015 to 2019," Environmental Pollution, vol. 317, Jan. 2023, doi: 10.1016/j.envpol.2022.120729.

[10] G. Tardy, E. Bideaux, C. Gostomski, and A. Fonseca, "Optimization Based Energy Efficient Power Transmission Design Methodology Applied to a Compact Excavator." [Online]. Available: https://hal.science/hal-04734340v1

[11] U. Uhanto, E. Yandri, E. Hilmi, R. Saiful, and R. Ariati, "Evaluating engine durability and operational effects of biodiesel blends in heavy equipment applications," Oct. 01, 2025, Elsevier B.V. doi: 10.1016/j.nxener.2025.100392.

[12] J. B. Heywood, Internal Combustion Engine Fundamentals, 2 (2018). New York: McGraw-Hill, 1988.

[13] M. Sheykhvazayefi, M. Gorji-Bandpy, A. Hajialimohammadi, and M. A. Mirsalim, "Experimental Study of the Coking Phenomenon Effects on Spray Characteristics of the High Pressure Diesel Injector," Journal of Applied Fluid Mechanics, vol. 13, no. 4, pp. 1117–1129, 2020, doi: 10.36884/jafm.13.04.30915.

[14] T. Cao, "Multifactorial mechanisms of cavitation and spray atomization in diesel injector nozzles: A comprehensive review," Dec. 01, 2025, SAGE Publications Inc. doi: 10.1177/16878132251405121.

[15] A. Y. Deshmukh, M. Davidovic, T. Grenga, R. Lakshmanan, L. Cai, and H. Pitsch, "A reduced-order model for turbulent reactive sprays in compression ignition engines," Combust. Flame, vol. 236, Feb. 2022, doi: 10.1016/j.combustflame.2021.111751.

[16] J. M. Desantes, R. Payri, F. J. Salvador, and A. Gil, "Development and validation of a theoretical model for diesel spray penetration," Fuel, vol. 85, no. 7–8, pp. 910–917, May 2006, doi: 10.1016/j.fuel.2005.10.023.

[17] J. K. Dukowicz, "A Particle-Fluid Numerical Model for Liquid Sprays*," 1980.

[18] M. Hawi, H. Kosaka, S. Sato, T. Nagasawa, A. Elwardany, and M. Ahmed, "Effect of injection pressure and ambient density on spray characteristics of diesel and biodiesel surrogate fuels," Fuel, vol. 254, Oct. 2019, doi: 10.1016/j.fuel.2019.115674.

[19] R. Payri, J. M. García-Oliver, G. Bracho, and J. Cao, "Experimental characterization of direct injection liquid ammonia sprays under non-reacting diesel-like conditions," Fuel, vol. 362, Apr. 2024, doi: 10.1016/j.fuel.2023.130851.

[20] M. Lapuerta, O. Armas, and J. Rodríguez-Fernández, "Effect of biodiesel fuels on diesel engine emissions," 2008, Elsevier Ltd. doi: 10.1016/j.pecs.2007.07.001.

[21] H. Wang, H. Hao, X. Li, K. Zhang, and M. Ouyang, "Performance of Euro III common rail heavy duty diesel engine fueled with Gas to Liquid," Appl. Energy, vol. 86, no. 10, pp. 2257–2261, 2009, doi: 10.1016/j.apenergy.2009.02.004.

[22] V. K. Gupta, Z. Zhang, and Z. Sun, "Modeling and control of a novel pressure regulation mechanism for common rail fuel injection systems," Appl. Math. Model., vol. 35, no. 7, pp. 3473–3483, Jul. 2011, doi: 10.1016/j.apm.2011.01.008.

[23] R. D. Reitz and G. Duraisamy, "Review of high efficiency and clean reactivity controlled compression ignition (RCCI) combustion in internal combustion engines," Feb. 01, 2015, Elsevier Ltd. doi: 10.1016/j.pecs.2014.05.003.

[24] F. Khusniawati and H. Palippui, “Analisis Perawatan Injector Akibat Penyumbatan Bahan Bakapr pada Main Engine Kapal,” Jurnal Inovasi Sains dan Teknologi Kelautan, no. 2, Jul. 2021, doi: https://doi.org/10.62012/zl.v1i2.10832.
[25] H. Hazar, R. Tekdogan, and H. Sevinc, “Determination of the effects of oxygen-enriched air with the help of zeolites on the exhaust emission and performance of a diesel engine,” Energy, vol. 236, no. X, p. 121455, 2021, doi: 10.1016/j.energy.2021.121455.
[26] A. M. Liaquat, H. H. Masjuki, M. A. Kalam, and I. M. Rizwanul Fattah, “Impact of biodiesel blend on injector deposit formation,” Energy, vol. 72, pp. 813–823, Aug. 2014, doi: 10.1016/j.energy.2014.06.006.
[27] S. Erdoğan, M. K. Balki, and C. Sayin, “The effect on the knock intensity of high viscosity biodiesel use in a DI diesel engine,” Fuel, vol. 253, pp. 1162–1167, Oct. 2019, doi: 10.1016/j.fuel.2019.05.114.
[28] R. D. Burke, M. Madamedon, and R. Williams, “Newly identified effects of injector nozzle fouling in diesel engines,” Fuel, vol. 278, Oct. 2020, doi: 10.1016/j.fuel.2020.118336.
[29] X. Zhu and Ö. Andersson, “Performance of new and aged injectors with and without fuel additives in a light duty diesel engine,” Transportation Engineering, vol. 1, Jun. 2020, doi: 10.1016/j.treng.2020.100007.
[30] C. Jiang et al., “Effect of fuel injector deposit on spray characteristics, gaseous emissions and particulate matter in a gasoline direct injection engine,” Appl. Energy, vol. 203, pp. 390–402, 2017, doi: 10.1016/j.apenergy.2017.06.020.
[31] Mokhtar et al., “Towards nationwide implementation of 40% biodiesel blend fuel in Indonesia: a comprehensive road test and laboratory evaluation,” Biofuel Research Journal, vol. 10, no. 3, pp. 1876–1889, 2023, doi: 10.18331/BRJ2023.10.3.2.